PCCP

Protein Mixtures of Environmental Friendly Zein to understand Protein – Protein Interactions through Biomaterials Synthesis, Hemolysis, and their Antimicrobial Activities

Journal:	*Physical Chemistry Chemical Physics*
Manuscript ID:	CP-ART-04-2014-001457.R1
Article Type:	Paper
Date Submitted by the Author:	20-May-2014

Complete List of Authors:	Bakshi, Mandeep Singh; WLU, Chemistry Mahal, Aabroo; DAV, Chemistry Kumar, Manoj; DAV, Chemistry Khullar, Poonam; DAV, Chemistry Kaur, Gurinder; CNA, Singh, Narinder; Indian Institute of Technology Ropar, Chemistry Kumar, Harsh; National Institute of Technology, Chemistry

Protein Mixtures of Environmental Friendly Zein to understand Protein – Protein Interactions through Biomaterials Synthesis, Hemolysis, and their Antimicrobial Activities

Aabroo Mahal[3,4], Manoj Kumar Goshisht[3,4], Poonam Khullar[3], Harsh Kumar[4], Narinder Singh[5], Gurinder Kaur[2], Mandeep Singh Bakshi[1]*

[1]Department of Chemistry, Wilfrid Laurier University, Science Building, 75 University Ave. W., Waterloo ON N2L 3C5, Canada, [2]Nanotechnology Research Laboratory, College of North Atlantic, Labrador City, NL A2V 2K7 Canada, [3]Department of Chemistry, B.B.K. D.A.V. College for Women, Amritsar 143005, Punjab, India, [4]Department of Chemistry, Dr. B. R. Ambedkar National Institute of Technology, Jalandhar-144011, Punjab, India. [5]Department of Chemistry, Indian Institute of Technology Ropar, Rupnagar-140001, Punjab, India.

First two authors have equal contribution.

Abstract

Industrial important zein protein has been employed to understand its interactions with two model proteins bovine serum albumin (BSA) and cytochrome c (Cyc,c) following the in vitro synthesis of Au NPs so as to expand its applicability for biological applications. Interactions were studied under the effect of temperature variation by using UV-visible and fluorescence emission studies. Temperature induced unfolding in the protein mixtures indicated their degree of mutual interactions through simultaneous nucleation of gold nanoparticles (Au NPs) and their subsequent shape control effects. Zein + BSA mixtures showed favorable protein – protein interactions over the entire mole fraction range with maximum close to x_{BSA} = 0.24, whereas zein + Cyc,c showed such interactions only in the zein rich region with significant demixing in the Cyc,c rich region of the mixtures. Both hydrophobic as well as hydrophilic domains in the unfolded states were driving such interactions in the case of zein + BSA mixtures while demixing was the result of predominantly hydrophilic nature of Cyc,c and its self-aggregation behavior in the Cyc,c rich region in contrast to the predominant hydrophobic nature

of zein. Zein + BSA mixtures produced small roughly spherical Au NPs fully coated with protein, whereas the demixing zone of zein + Cyc,c mixture generated highly anisotropic NPs with little protein coating. To explore their biological applications, protein conjugated NPs of both mixtures were subjected to hemolysis where NPs coated with the former mixture showed little hemolysis and may act as drug delivery vehicles in systemic circulation in comparison to the latter. Both kinds of NPs further demonstrated their extraordinary antimicrobial activities with different kinds of strains and proved to be highly important environmental friendly biomaterials.

Key words: Protein – protein interactions, zein protein, biomaterials, hemolysis.

Corresponding Author

*E-mail: ms_bakshi@yahoo.com

Introduction

Protein – protein interactions[1-4] is most important tool in understanding the fundamental basis of biophysical chemistry. Most of the biological functions involving biochemical processes are closely controlled by the protein – protein interactions. Signal transduction is one of the most important biological processes which play a significant role in several tumors. Usually multi-protein complex performs several catalytic functions which are not in the preview of its components. Protein – protein interactions are involved in almost every biochemical process in a living cell. Information about these interactions is essential for the development of new therapeutic approaches toward different diseases as well as for their environmental applications. Here, we are presenting a simple and straight forward method in exploring such interactions by taking the advantage of gold (Au) nanoparticles (NPs) synthesis in vitro in the presence of a binary combination of proteins,[5-10] where growing NPs act as sensors for such interactions. We show that bioconjugated NPs thus produced depict the properties of the protein complexes and hence best suited for drug delivery vehicles as well as antimicrobial agents.

The synthesis of Au NPs can be easily achieved through the reduction of Au(III) into Au(0) by electron donating amino acids such as cysteine.[9] For an effective reduction process, cysteine has to be aqueous exposed by breaking the disulfide bonds which are usually buried

deep in the secondary structure of a protein and hence protein needs to be in the unfolded state.[9] The unfolded form is highly prone to protein – protein interactions in comparison to the folded form due to aqueous exposed hydrophilic as well as hydrophobic domains which can easily interact with the respective domains of another protein. Usually, unfolding and seeding are the most important factors[11-13] which promote such interactions and can be easily followed through the in vitro synthesis of Au NPs. The latter is highly facilitated by protein unfolding process[14] and thus provides direct indication of unfolding behaviour. Unfolded protein simultaneously adsorbs on the NP surface and hence, triggers the seeding with the folded or unfolded forms[9] of aqueous solubilised protein to generate protein – protein interactions.[15]

Zein is highly important industrial and environmental friendly alcohol soluble corn storage protein with extensive food applications. It is clear, odorless, tasteless, edible, and hence used in processed foods and pharmaceuticals. It contains high proportions of non-polar amino acid residues (such as leucine, alanine, and proline) which render it water insoluble.[16,17] Since zein is completely safe to ingest, it is used for perfect coating of foods and pharmaceutical ingredients, and hence it interacts with other proteins upon its way to ingestion. Understanding interactions of zein with BSA and Cyc,c as model proteins will pave the way for its better applicability in pharmaceutical industry as well as its environmental applications. Zein is predominantly hydrophobic protein and possesses a highly robust structure which is made up of nine homologous repeat units arranged in an anti-parallel distorted cylindrical form and stabilized by the hydrogen bonds.[18-20] In order to understand its interactions with other water soluble proteins, it has to be solubilized in the aqueous phase. Its solubility can be achieved in aqueous surfactant solution where surfactant molecules interact with its hydrophobic domains and thus allow its hydrophilic domains to interact with the aqueous phase to facilitate its solubilization.[20] Once in the solubilized form, it is expected to interact with other water soluble proteins through polar as well as non-polar interactions. Since, it is one of the most promising proteins to produce bioconjugated Au NPs[10], therefore, NPs conjugated with its complexes with other proteins are also expected to have the same ability but with better functionalities in terms of biological applications such as drug delivery vehicles where protein complexes play a better role. In addition, since zein is frequently used in the food products, therefore, antimicrobial properties of such NPs are equally important to explore.

Experimental

Materials

Chloroauric acid ($HAuCl_4$), zein protein (molar mass 21 kDa), bovine serum albumin (BSA) (molar mass 66 kDa), cyctochrome c (Cyc,c) (molar mass 12 kDa) from bovine heart muscle, and sodium dodecylsulfate (SDS) were purchased from Aldrich. Double distilled water was used for all preparations. Zein was aqueous solubilized by taking 24 mM SDS solution.

In vitro synthesis of Au NPs in protein – protein binary mixtures

Binary mixtures of zein + BSA and zein + Cyc,c were made by taking 10 mg/10 ml of each protein solution. Then, a desired amount of $HAuCl_4$ (0.25 – 1.0 mM) was added in 10 ml of each solution in screw-capped glass bottles and kept in water thermostat bath (Julabo F25) at precise 70 ± 0.1 ^oC for six hours under static conditions. Protein mixture especially in the unfolded state induced by the high temperature[8-10] initiated the reduction of Au(III) into Au(0) due to its weak reducing ability and resulted in the color change from colorless to pink-purple. After six hours, the samples were cooled to room temperature and kept for overnight. They were purified from pure water at least three times to remove unreacted protein. Purification was done by collecting the Au NPs at 8,000 – 10,000 rpm for 5 min after washing each time with distilled water. These reactions were also simultaneously monitored under the effect of temperature variation from 20 – 70 ^oC with UV-visible (Shimadzu-Model No. 2450, double beam) and steady state fluorescence spectroscopy (PTI QuantaMaster) measurements in the wavelength range of 200 – 900 nm to observe the influence of protein complex on the synthesis of Au NPs in terms of protein unfolding. Both instruments were equipped with a TCC 240A thermoelectrically temperature controlled Cell Holder that allowed to measure the spectrum at a constant temperature within ± 1^oC. Au NPs were characterized by Transmission Electron Microscopic (TEM) analysis on a JEOL 2010F at an operating voltage of 200 kV. The samples were prepared by mounting a drop of a solution on a carbon coated Cu grid and allowed to dry in the air.

Hemolytic assay

Hemolytic assay was performed to evaluate the response of protein-conjugated NPs on blood group B of red blood cells (RBCs) from a healthy human donor. Briefly, 5% suspension of

RBCs was used for this purpose after giving three washings along with three concentrations (i.e. 25, 50, and 100 μg/ml) of each NPs sample. 1 ml packed cell volume (i.e. hematocrit) was suspended in 20 ml of 0.01 M phosphate buffered saline (PBS). The positive control was RBCs in water and it was prepared by spinning 4 ml of 5% RBCs suspension in PBS. PBS as supernatant was discarded and pellet was resuspended in 4 ml of water. The negative control was PBS. All the readings were taken at 540 nm i.e. absorption maxima of hemoglobin.

Microbiological evaluation

Antifungal activities of bioconjugated NPs were evaluated using disc-diffusion test for pre-screening of antifungal potential of agents and the broth micro-dilution method to determine the minimum inhibitory concentration (MIC). The following fungal strains were used; Asperagillus niger (MTCC-281), Candidum geotrichum (MTCC-3993), Candida albicans (MTCC-227) and Candida tropicalis (MTCC-230). Fungi were cultivated at 25 ^{o}C on Sabouraud Dextrose Agar (SDA) and MIC was determined by using Sabouraud Dextrose Broth (SDB). The samples and standard were suspended in dimethylsulfoxide (DMSO, 1/10) and applied in different concentrations. DMSO was used as a negative control and antifungal (fluconazole) as positive controls.

Antifungal activity

The disk-diffusion assay was applied to determine the growth inhibition of fungi by protein conjugated NPs. Overnight fungal cultures (100 μL) were spread onto SDA. The NPs sampls were applied to 8 mm disks (Whatman paper No.1). After 48 h of incubation at 25 ^{o}C, the diameter of growth inhibition zones was measured.

MIC determination

The broth dilution test was performed in test tubes. The conidial suspension, which gave the final concentration of 1 x 10^5 CFU/ml, was prepared. A growth control tube and sterility control tube were used in each test. After 24-72 h incubation at 25 ^{o}C, the MIC was determined visually as the lowest concentration that inhibits growth, evidenced by the absence of turbidity.

Results and discussion

Interactions between the components of Zein + BSA binary mixtures

Interactions between zein and BSA are studied by following the synthesis of Au NPs. Fig 1a shows a typical reaction of the synthesis of Au NPs in an aqueous mixture of zein + BSA with mole fraction of BSA, $x_{BSA} = 0.24$ under the effect of temperature variation. For comparison, the same reaction under identical conditions without gold salt is depicted in the inset. This reaction shows a single peak around 280 nm mainly due to the tryptophan, tyrosine (Tyr), and phenylalanine (Phe) residues of both proteins (zein is deficient in tryptophan), which remains unaffected with the temperature variation from 20 – 70 ^{o}C. In contrast, in the presence of gold salt (Fig 1a), this peak disappears and another prominent peak appears around 310 nm due to the formation of ligand to metal charge transfer complex (LMCT)[21-23] between the electron donating amino acids and the electropositive metal centre of $AuCl_4^-$ ions which results in the reduction of Au(III) to Au(0) to produce Au NPs. This is carried out only by the unfolded form of protein as explained in our previous work[8-10] and is simultaneously indicated by the appearance of an absorbance at 540 nm due to the surface plasmon resonance (SPR) of Au NPs. Similar reactions are done over the whole mole fraction range and some of the reactions are shown in *Supporting information, Fig S1*. LMCT peak at 310 nm decreases whereas absorbance of Au NPs at 540 nm increases with temperature, and their variation is shown in Fig 1b. There is a marked decrease in the 310 nm peak (empty diamonds) up to 44 ^{o}C due to the consumption of LMCT complex into Au nucleating centres,[24,25] thereafter it passes through a weak hump from 44 to 56 ^{o}C before decreasing further up to 70 ^{o}C. Meanwhile, 540 nm peak (filled diamonds) gradually increases and demonstrates an inflection point around 50 ^{o}C. It is accompanied with a significant red shift of ~32 nm (filled circles) within a temperature range of 44 – 56 ^{o}C due to the inter-particle fusion of nucleating centres to produce NPs which subsequently grow in size with further rise in the temperature. Therefore, 44 ^{o}C is in fact the nucleation temperature (N_T, see Fig 1b) which initiates the conversion of tiny nucleating centres into NPs and this transition goes through a broad inflection in the 540 nm absorption peak within 44 – 56 ^{o}C (shown as a shaded area).

Likewise, Fig 1c demonstrates the fluorescence emission of tryptophan (mainly due to BSA) and, Tyr and Phe (mainly due to zein) residues[26-28] of this mixture ($x_{BSA} = 0.24$) at 308 nm when excited at 280 nm in the presence of gold salt under the temperature variation of 20 – 70

^{o}C. "Blank" scan represents the protein solution before adding gold salt while the addition of gold salt induces significant quenching in the emission. Same reaction in the absence of gold salt is depicted in the inset. In both cases, the emission at 308 nm is influenced by the zein rather than the BSA because only pure zein shows the emission at 308 nm (*Fig S2*) rather than pure BSA (340 nm) (*Fig S2*). It attributes to the drastic change in the environment of tryptophan when BSA is mixed with zein, or in other words tryptophan is entirely engulfed by the predominantly hydrophobic domains of zein resulting in a significant blue shift[29,30] from 340 to 308 nm with the consequence emission of tryptophan is merged with that of Tyr and Phe. This is systematically shown in *Fig S3* by adding zein to aqueous BSA in the absence of gold salt. The variation in fluorescence intensity of 308 nm emission peak of x_{BSA} = 0.24 in the presence and absence of gold salt from Fig 1c is extracted and plotted in Fig 1d. It is also compared with the emission from individual BSA and zein in the presence of gold salt. In the absence of gold salt, the fluorescence emission of x_{BSA} = 0.24 linearly decreases with temperature[31,32] due to the successive unfolding of zein + BSA complex which aqueous exposes the fluorescence active residues. In contrast, in the presence of gold salt, emission goes through a strong maximum in each case and is caused by an increase in the non-polar environment sensed by the fluorescent active residues due to the neutralization of the protein surface charge[33,34] by the adsorption of $AuCl_4^-$ ions which induces conformational changes. A decrease in the emission thereafter is due to the unfolding of the protein that aqueous exposes these residues and induces fluorescence quenching. In addition, the unfolded form also simultaneously stabilizes the growing Au NPs by surface adsorption and hence undergoes fluorescence quenching. Thus, the maximum in the curve which corresponds to 40 ^{o}C can be taken as the unfolding temperature (U_T) of zein + BSA complex at x_{BSA} = 0.24 (Fig 1d), which is slightly lower than the N_T = 44 ^{o}C of Fig 1b because unfolding in fact initiates the nucleation to produce Au NPs by aqueous exposing reducing amino acids like cysteine.[8] Similar correlation between the N_T and U_T from UV-visible and fluorescence studies, respectively, has been observed at other mole fractions, and the fluorescence behavior of some of them is shown in *Fig S4*.

Both U_T and N_T thus computed over the whole mole fraction range are plotted in Fig 2a. Since unfolding triggers the nucleation and also stabilizes the growing NPs[8-10], therefore, nucleation also follows the unfolding. It indicates that the unfolding of zein + BSA mixtures at

different mole fractions is happening at much lower temperature in comparison to the ideal mixing (dotted line) and is maximum at x_{BSA} = 0.24 between zein and BSA. Occurrence of the unfolding at lower temperatures than the ideal mixing between the components of zein and BSA can also be viewed as their favorable complexation which further promotes their mutual unfolding. We expect a similar behavior when reactions are conducted at constant temperature of 70 ^{o}C, where both proteins are already in their fully unfolded forms.[8,10] Fig 2b shows a reaction profile of UV-visible measurements with time for a reaction at x_{BSA} = 0.24, while similar reactions at some other mole fractions are shown in *Fig S5*. Plots of intensity of 540 nm absorbance versus reaction time for different mole fractions are depicted in Fig 2c. In each case, synthesis of the Au NPs begins within 1 minute of the reaction time, because both proteins as well as their complexes are already in the fully unfolded form and hence demonstrate maximum reduction potential.[8-10] Nucleating centres thus created undergo an instant growth process which is indicated by a sharp rise in the 540 nm absorbance. After certain reaction time absorbance tends to constant signaling the completion of the growth process. The time required for the completion has been calculated for each mole fraction from the inflection point in each curve as demonstrated for few plots in Fig 2c, and plotted in Fig 2d over the entire mole fraction range. Interestingly, this plot also shows almost similar trend to that of Fig 2a, and x_{BSA} = 0.24 takes minimum reaction time to complete the reaction. The minimum time can further be related to the maximum unfolding of zein + BSA complex which possesses maximum reduction potential[8] by aqueous exposing the cystein residues to complete the reaction in minimum time. Thus, both figures come to a common conclusion that zein and BSA undergo marked unfolding due to maximum protein – protein interactions close to x_{BSA} = 0.24 which simultaneously facilitates the nucleation with respect to the reaction temperature (Fig 2a) as well as time (Fig 2d).

Microscopic studies (Au NPs + Zein + BSA)

TEM studies have been performed to demonstrate the correlation between the unfolding of zein + BSA complex and the nucleation of Au NPs because the colloidal stabilization of NPs is achieved by the surface adsorption of unfolded protein due to its amphiphilic nature. TEM images of some of the samples synthesized at different mole fractions have been shown in Fig 3. Fig 3a depicts the TEM image of Au NPs of 20 ± 7 nm prepared with x_{BSA} = 0 (i.e. only zein).

Aggregates of Au NPs completely wrapped by the unfolded zein are evident and similar results have already been reported for other water soluble proteins where such proteins have been employed for in vitro synthesis of Au NPs.[8-10] However, a good comparison can be made by comparing the uncoated citrate stabilized Au NPs prepared under similar experimental conditions without protein and are shown in *Fig S6*. The uncoated NPs are relatively much smaller in size (8 ± 5 nm) and completely lack protein coating since citrate provides colloidal stability rather than the shape control effects. In addition, sodium citrate is an electrolyte in contrast to polymeric protein, and hence protein adsorption is viewed as a thick coating on the NP surface as one can see in Fig 3, which is not the outcome of any sort of artifacts as well as other unwarranted impurities. Fig 3b shows a close up image of the sample prepared with x_{BSA} = 0.17, where a thick layer of protein coating is clearly visible (indicated by a block arrow). Thick protein coating is also visible for the Au NPs prepared with x_{BSA} = 0.24 (Fig 3c,d) as well as with x_{BSA} = 0.56 (Fig 3e,f) suggesting an active involvement of protein mixtures in the NP stabilization as well as its shape control effects which produces mostly roughly spherical morphologies of 20 – 30 nm. Thus, nucleation is facilitated as well as closely controlled by the adsorption of unfolded protein on the NP surface which further promotes the protein seeding and hence accelerates protein – protein interactions.[35-37]

Interactions between the components of Zein + Cyc,c binary mixtures

Mixing behavior of zein + Cyc,c is relatively much complicated to follow because of the presence of Soret and Q-band of Cyc,c. UV-visible scans of $x_{Cyc,c}$ = 0.53 without and with gold salt in the temperature range of 20 to 70 ^{o}C are depicted in Fig 4a and b, respectively. Three prominent peaks (as indicated by arrows) at 280 nm (due to tryptophan, Tyr, or Phe), 400 nm (Soret band of Cyc,c), and 520 nm (Q band of Cyc,c) are evident in Fig 4a which remain almost unaffected. However, in the presence of gold salt (Fig 4b), all peaks are significantly affected with the appearance of a new band at 540 nm due to the SPR of growing Au NPs which overshadows the Q band of Cyc,c at 520 nm. Soret band at 400 nm blue shifts to 385 nm, while 280 nm peak bifurcates to generate a broader band around 310 nm again due to the LMCT complex formation as observed previously in Fig 1a for zein + BSA mixture. The bifurcation of 280 nm peak is due to the involvement of zein or zein + Cyc,c in the LMCT complex formation

(see *Fig S7*, for LMCT in pure zein) rather than Cyc,c, because Cyc,c does not show the LMCT formation (*Fig S7*). This is probably due to the greater affinity of Cyc,c to involve in the electron exchange reaction in comparison to zein which results in an instant reduction of Au(III) into Au(0) without going through an LMCT formation. The variation in 310 nm, 385 nm, and 540 nm peaks for $x_{Cyc,c} = 0.53$ from Fig 4b is illustrated in Fig 4c. Intensity of both 310 nm and 385 nm peaks regularly decreases with the rise in temperature and eventually disappears around 36 ^{o}C, where the absorbance due to the SPR of Au NPs becomes prominent. Therefore, 36 ^{o}C is the N_T, where nucleation sets in among the nucleating centres to produce Au NPs and they are simultaneously stabilized by the protein as demonstrated in Fig 1b for zein+BSA mixture. Disappearance of 310 nm peak clearly indicates the consumption of LMCT into Au NPs, while that of 385 nm peak of Soret band is due to the heme degradation in the event of protein unfolding and loss of tertiary structure.[38] This happens due to the covalent interactions with the NP surface, because the heme is covalently linked to the protein through thioether bridges between the vinyl groups of the heme and the sulfur atoms of two cysteine side-chains. Thus, surface adsorption not only leads to a change in the symmetry[38] of the heme group but also induces conformation changes with the result absorbance of the Soret band is eliminated.

UV-visible results have been further supplemented from the emission studies. Fig 4d shows the emission spectrum of this reaction (i.e. $x_{Cyc,c} = 0.53$). A prominent peak at 308 nm traced by the dotted line is due to the emission of fluorescence active residues (tryptophan, Tyr, or Phe) of zein + Cyc,c mixture in the absence of gold salt (blank). Addition of gold salt induces significant quenching which further depends on the temperature variation. The same reaction without gold salt also shows a prominent peak at 308 nm (*Fig S8a*). Again 308 nm peak is mainly due to zein (see the emission spectrum of pure zein in *Fig S2*) because tryptophan emission of pure Cyc,c occurs around 340 nm (*Fig S8b*) and is supposed to be blue shifted and merged with 308 nm peak in the event of zein + Cyc,c complexation as observed for zein + BSA mixture in *Fig S3*. The variation in the emission intensity of 308 nm peak in the presence and absence of gold salt for zein + Cyc,c mixtures with $x_{Cyc,c} = 0.53$ is shown in Fig 5a. In the absence of gold salt, it shows a linear relation with temperature, as temperature aqueous exposes the fluorescence active residues and hence converts the radiative decay into non-radiative decay due to a successive increase in the intermolecular collisions, while in the presence of gold salt, it

goes through a strong maximum much like the same way as observed for zein + BSA mixture in Fig 1d. Again the maximum in the emission curve represents the unfolding temperature, U_T, of zein + Cyc,c complex as discussed previously for Fig 1d.

Both N_T (from Fig 4c) and U_T (from Fig 5a) values thus evaluated from the UV-visible and fluorescence studies, respectively, have been collectively plotted in Fig 5b over the entire mole fraction range of zein + Cyc,c mixtures. N_T values show negative deviation from the ideal behavior and it is minimum around $x_{Cyc,c} = 0.53$. In other words, this mole fraction is possessing maximum reduction potential to initiate the reaction at lowest temperature in comparison to other mole fractions. Maximum reduction potential is obviously demonstrated by the maximum unfolding due to stronger interactions between the components of zein + Cyc,c mixture. Likewise, the U_T values especially in the zein rich region of the mixture show good correlation with the N_T because unfolding essentially triggers the nucleation of Au NPs. However, no correlation is observed in the Cyc,c rich region, where U_T departs from N_T and decreases linearly with the increase in the amount of Cyc,c in zein + Cyc,c mixtures. It seems that there is demixing[39-41] in the Cyc,c rich region where the excessive amount of unfolded Cyc,c which is not involved in the complexation with zein, remains in the solution. This is also evident from the bifurcated UV peaks at 280 nm and 310 nm representing the tryptophan from mainly uncomplexed Cyc,c and LMCT from zein + Cyc,c complex absorptions (Fig 4b), respectively. The origin of demixing[39-41] can be attributed to the predominantly highly hydrophilic nature of Cyc,c and also its tendency to undergo self-aggregation[42] leading to the formation of micelle like assemblies[14]. In the Cyc,c rich region, once the zein is complexed to form a stable zein + Cyc,c complex, the extra amount of Cyc,c follows the self-aggregation and hence its unfolding behavior does not follow the nucleation of Au NPs.

Microscopic studies (Au NPs + Zein + Cyc,c)

TEM images of Au NPs produced in the presence of binary mixtures of zein + Cyc,c are shown in Fig 6, which show contrasting differences from that of Fig 3. Fig 6a represents the TEM micrograph of a sample prepared with $x_{Cyc,c} = 0.16$. Most of the NPs are flat triangle of 83±17 nm size along with much smaller faceted NPs of different shapes, and no protein coating is visible, while corresponding mixture of zein+BSA (Fig 3b) produced mostly roughly spherical

shapes of much smaller size with substantial surface coating. However, increase in the mole fraction ($x_{Cyc,c}$ = 0.53) induces some degree of anisotropy that leads to the shape deformation (Fig 6b), but as it shifts to the Cyc,c rich region of the mixture ($x_{Cyc,c}$ = 0.73), substantial anisotropic growth is observed and NPs acquire dendritic shapes[43,44] indicating significant decrease in the shape control behavior of this mixture (Fig 6c,d). Further increase in the mole fraction ($x_{Cyc,c}$ = 0.87) even produces larger aggregates of dendritic growth with practically no shape control effects (Fig 6e,f). This is in contrast to much smaller NPs produced in the BSA rich region of the mixture (Fig 3e,f). Thus, the unfolded form of Cyc,c rich region of the mixtures completely lack the surface adsorption as demonstrated by Fig 5b with no correlation between the U_T and N_T, and hence no shape control effects are observed. It further supports our earlier conclusion that extra amount of Cyc,c remains in the solution due to the self aggregation[14] tendency of Cyc,c which is considered to be the driving force for keeping the uncomplexed Cyc,c in the aqueous phase. Thus, uncomplexed Cyc,c is not involved in the NPs stabilization or shape controlled effects with the results highly anisotropic morphologies emerge.

Mechanism of protein – protein interactions

Above results help us to understand that zein has stronger interactions with BSA rather than Cyc,c and that too in the zein rich region of both mixtures (Fig 2a and 5b). Such interactions[4] are driven by the electrostatic (hydrogen bonds, ionic interactions) as well as non-electrostatic (Van der Waals forces or hydrophobic bonds) forces and further related to the size, shape, complementarity between surfaces, and conformational changes on complex formation between different proteins. Since the unfolded forms of different proteins in present mixtures are involved in the complexation, therefore, the complex formation is the consequence of highly stable and non-transient interactions. Because of highly hydrophobic nature of zein, it is solubilized in the aqueous SDS solution which allows the zein to acquire a net negative charge[20] (see the displacement of protein coated NPs towards the +ive terminal of the battery, *Fig S9*). The extent of solubilization is related to the amount of SDS used. Greater amount of SDS induces greater solublization and hence greater unfolding of the zein.[20] Thus, total amount of SDS used in this study is expected to exist only in the complexed state with zein. Therefore, there is little possibility of its monomeric form to interact with BSA or Cyc,c to induce any

significant amount of conformation changes. Thus, the negative charge acquired by the zein due to its complexation with SDS predominantly drives the electrostatic interactions with hydrophilic domains of BSA and Cyc,c. On the other hand, acidic reaction pH (~ 2.5, due to the presence of H^+ ions from the dissociation of $HAuCl_4$) induces the net positive global charge on the BSA (isoelectric point, pI = 4.7) and Cyc,c (pI = 10) macromolecules which triggers the electrostatic interactions with negatively charged zein (Fig 7a,b). The resulting complex in both mixtures is still predominantly negatively charged because all negative sites of zein are not neutralized by BSA or Cyc,c even in their respective rich regions of the mixtures (see *Fig S9* and *S10,* where NPs of all samples move toward +ive terminal), and hence the complexation is also driven by other non-electrostatic interactions which arise from the non-polar domains of different proteins.

Zein is predominantly hydrophobic in nature, hence participation of its hydrophobic domains in the complexation cannot be ruled out. However, much larger size (see molar masses in the experimental section), shape, and surface area of unfolded BSA in comparison to unfolded Cyc,c possesses a non-polar domain of greater hydrophobic potential which is expected to trigger the hydrophobic interactions with the hydrophobic domains of zein. This is evident from Fig 2a,d with minimum lying in the zein rich region (x_{BSA} = 0.24) where smaller sized zein in comparison to BSA has greater amount to have maximum hydrophobic interactions in the form of 2:1 complex as shown in Fig 7c. This complex brings down the N_T to minimum value due to better surface adsorption with stronger amphiphilic nature in comparison to other stochiometries. The reason of attaining this stoichiometry can be related to several factors such as complementarity, conformational changes, and steric compulsions which allow achieving the maximum stability in the form of 2:1 stoichiometry in order to satisfy both the hydrophilic as well as hydrophobic interactions. In contrast, much smaller predominantly hydrophilic Cyc,c shows mainly electrostatic interactions with almost double sized predominantly hydrophobic zein in the zein rich region of the mixture (Fig 5b), and promotes the self-aggregation[42] (Fig 7d) and resulting demixing in the Cyc,c rich region. A large charge disparity between Cyc,c and zein is considered to be the main reason for 1:1 complexation in contrast to 2:1 for zein and BSA, and hence primarily responsible for the promotion of self – aggregation of Cyc,c in its rich region of the mixture.

Hemolysis

Here, we want to explore the possibility of protein complex coated NPs as drug release vehicles in systemic circulations and hence their hemolytic assay is important to understand. Uncoated Au NPs have been found to have significant interactions with the cell wall of the blood cell which causes hemolysis.[45] While, small mesoporous silica NPs (~100 nm) cause little hemolysis in comparison to larger ones which induce a strong local membrane deformation leading to hemolysis.[46] However, protein coated Au NPs significantly reduce the hemolytic effect in comparison to uncoated NPs.[10] Thus, the degree of hemolysis can be directly related to the protein coating of NPs.

Results of hemolysis of Au NPs prepared over the entire mole fraction range of both mixtures were tested and are presented in percentage hemolysis = **(**sample absorbance - negative control absorbance**)/(**positive control absorbance-negative control absorbance**) x** 100. Fig 8a shows typical absorbance profiles of different doses of a purified sample along with the positive and negative controls. The absorbance profile in each case is typical of hemoglobin with no interference from Cyc,c which does not show such a symmetric patter close to 540 and 575 nm (see *Fig S7*). Fig 8b illustrates the variation in the hemolysis of all samples of both mixtures. A clear difference between the sets of data for zein + BSA and zein + Cyc,c is evident. Three doses of zein + BSA conjugated NPs (i.e. 25, 50, and 100 μg/ml) show almost insignificant hemolysis with little difference, whereas zein + Cyc,c coated Au NPs show pronounced hemolysis in the Cyc,c rich region of the mixture which further depends on the dose of NPs. Significant hemolysis is the consequence of several factors[46,47] which include highly anisotropic dendritic growth with large surface area and practically little protein coating (Fig 6). This allows the hemolysis by the dendritic NPs a thermodynamic favorable process to interact with the cell membrane through predominantly naked metal surface (Fig 8c). Thus, greater number of NPs as of 100 μg/ml with least protein coating shows maximum hemolysis in comparison to smaller doses. This proves the close correlation between the NP stabilization by the protein surface adsorption and hemolysis. Complexation of BSA with zein renders the hydrophobic interactions of zein ineffective to disrupt the blood cell membrane through non-polar interactions and that is why little hemolysis is observed for zein + BSA mixtures. Thus, zein + BSA coated NPs is

considered to be the better model for its role as drug release vehicles in comparison to zein + Cyc,c coated NPs. Likewise, other protein combinations where more than one protein is required for biomedical applications can be tested and implemented in biological formulations.

Antimicrobial studies

Wide applicability of zein in food and pharmaceutical industry prompted us to investigate the antimicrobial activities of the present protein coated NPs. This is mainly to improve the shelf life of the pharmaceutical formulations of such NPs. Four kinds of strains (see experimental) have been selected for this study. *Aspergillus niger* is a common contaminant of food and is usually present in indoor environments. If its spores are inhaled in large amount, it causes serious lung disease. Interestingly, it plays a vital role in the solubilization of heavy metal sulfides[48] where metal ions interact with its cell wall. *Geotrichum candidum* is a plant pathogen which is found in many different sources from dairy products to soils. *Candida albicans* is a kind of yeast which causes oral and genital infections in humans,[49] and is normally present in the gut flora as a symbiotic agent. Its overgrowth results in yeast infection. *Candida tropicalis* is a common medical yeast pathogen, which has been implicated in infections of patients with neutropenia. We tested our Au NPs samples prepared over the entire mole fraction of zein + BSA and zein + Cyc,c mixtures for their antimicrobial activities against these four strains and the results are presented in Fig 9a and b, respectively. A dotted red line in both figures represents minimum inhibitory concentration (MIC)[50,51] of an antifungal (fluconazole) as control. Fluconazole is a drug used in the treatment and prevention of superficial and systemic fungal infections. In comparison to this drug though all the samples of protein conjugated NPs need much higher MIC, the concentration range in micrograms allows us to put them in the category of moderately antifungal agents. This is certainly an advantage in addition to their role in the pharmaceutical formulations where antimicrobial activities help us to improve their functionalities against the common yeast infections as well as their shelf life.

Conclusions

The present results conclude that zein demonstrates strong interactions with BSA throughout the mole fraction range whereas such interactions are limited to the zein rich region

with Cyc,c. BSA interacts with zein through both electrostatic as well as hydrophobic interactions whereas Cyc,c predominantly demonstrate electrostatic interactions. Both zein + BSA as well as zein + Cyc,c complexes simultaneously adsorb on the growing Au NPs and hence they control their shape evolution with the result mostly spherical NPs are produced in the former case while poor coating of the latter generated large dendritic NPs. Since zein is industrial protein, therefore its complexes with BSA and Cyc,c coated NPs have been explored for pharmaceutical as well as food applications. The Au NPs coated with zein + BSA complex prove to be fine vehicles for drug release in systemic circulation because of their negligible hemolysis almost throughout the whole mole fraction range. This is not the case with zein + Cyc,c complex coated NPs, which show significant hemolysis in the Cyc,c rich region. Interestingly, NPs coated with the complexes of both mixtures show almost same degree of antimicrobial activities against four prominent strains which are frequently available in the food products and cause yeast infections. Hence, the formulations made of such protein coated NPs have dual advantages as drug release vehicles and antimicrobial activities which is usually a rare combination for a formulation for biological applications.

Acknowledgment: These studies were partially supported by financial assistance under Article 27.9 of the CAS agreement of WLU, Waterloo, and from CSIR [ref no: 01(2683)/12] and DST [ref no: SR/FT/CS-28/2011], New Delhi. Dr Gurinder Kaur thankfully acknowledges the financial support provided by the Research and Development Council (RDC) of Newfoundland and Labrador, NSERC, and the Office of Applied Research at CNA. P.K. acknowledges the TEM studies done by SAIF Lab, Nehu, Shillong.

Supporting Information Available: UV-visible and fluorescence spectra are available free of charge via the Internet. This information is available free of charge via the Internet.

References

1. Oncley, J. L.; Ellenbogen, E.; Gitlin, D.; Gurd, F. R. N. Protein–Protein Interactions. *J. Phys. Chem.* **1952,** *56,* 85-92.

2. Rakickas, T.; Gavutis, M.; Reichel, A.; Piehler, J.; Liedberg, B.; Valiokas, R. à. Protein–Protein Interactions in Reversibly Assembled Nanopatterns. *Nano Lett.* **2008,** *8,* 3369-3375.

3. Elcock, A. H.; Sept, D.; McCammon, J. A. Computer Simulation of Protein–Protein Interactions. *J. Phys. Chem. B* **2001,** *105,* 1504-1518.

4. del Pino, P.; Pelaz, B.; Zhang, Q.; Maffre, P.; Nienhaus, G. U.; Parak, W. J. "Protein corona formation around nanoparticles - from the past to the future", *Materials Horizon* **2014**, in press.

5. Hattori, T.; Umetsu, M.; Nakanishi, T.; Sawai, S.; Kikuchi, S.; Asano, R.; Kumagai, I. A High-Affinity Gold-Binding Camel Antibody: Antibody Engineering for One-Pot Functionalization of Gold Nanoparticles As Biointerface Molecules. *Bioconjugate Chem.* **2012,** *23,* 1934-1944.

6. Manikas, A. C.; Causa, F.; Della Moglie, R.; Netti, P. A. Tuning Gold Nanoparticles Interfaces by Specific Peptide Interaction for Surface Enhanced Raman Spectroscopy (SERS) and Separation Applications. *ACS Appl. Mater. Interfaces* **2013,** *5,* 7915-7922.

7. Burt, J. L.; Gutirrez-Wing, C.; Miki-Yoshida, M.; Jos-Yacamín, M. Noble-Metal Nanoparticles Directly Conjugated to Globular Proteins. *Langmuir* **2004,** *20,* 11778-11783.

8. Bakshi, M. S.; Kaur, H.; Khullar, P.; Banipal, T. S.; Kaur, G.; Singh, N. Protein Films of Bovine Serum Albumin Conjugated Gold Nanoparticles: A Synthetic Route From Bioconjugated Nanoparticles to Biodegradable Protein Films. *J. Phys. Chem. C* **2011,** *115,* 2982-2992.

9. Bakshi, M. S. Nanoshape Control Tendency of Phospholipids and Proteins: Protein–Nanoparticle Composites, Seeding, Self-Aggregation, and Their Applications in Bionanotechnology and Nanotoxicology. *J. Phys. Chem. C* **2011,** *115,* 13947-13960.

10. Mahal, A.; Khullar, P.; Kumar, H.; Kaur, G.; Singh, N.; Jelokhani-Niaraki, M.; Bakshi, M. S. Green Chemistry of Zein Protein Toward the Synthesis of Bioconjugated Nanoparticles: Understanding Unfolding, Fusogenic Behavior, and Hemolysis. *ACS Sustainable Chem. Eng.* **2013,** *1,* 627-639.

11. Bolder, S. G.; Sagis, L. M. C.; Venema, P.; van der Linden, E. Effect of Stirring and Seeding on Whey Protein Fibril Formation. *J. Agric. Food Chem.* **2007,** *55,* 5661-5669.

12. Men, D.; Guo, Y. C.; Zhang, Z. P.; Wei, H. p.; Zhou, Y. F.; Cui, Z. Q.; Liang, X. S.; Li, K.; Leng, Y.; You, X. Y.; Zhang, X. E. Seeding-Induced Self-Assembling Protein Nanowires Dramatically Increase the Sensitivity of Immunoassays. *Nano Lett.* **2009,** *9,* 2246-2250.

13. Shaw Stewart, P. D.; Kolek, S. A.; Briggs, R. A.; Chayen, N. E.; Baldock, P. F. M. Random Microseeding: A Theoretical and Practical Exploration of Seed Stability and Seeding Techniques for Successful Protein Crystallization. *Crystal Growth & Design* **2011,** *11,* 3432-3441.

14. Bakshi, M. S.; Kaur, H.; Banipal, T. S.; Singh, N.; Kaur, G. Biomineralization of Gold Nanoparticles by Lysozyme and Cytochrome c and Their Applications in Protein Film Formation. *Langmuir* **2010,** *26,* 13535-13544.

15. Zhang, D; Neumann, O.; Wang, H.; Yuwono, V. M.; Barhoumi, A.; Perham, M.; Hartgerink, J. D.; Wittung-Stafshede, P.; Halas, N. J. *Nano Lett*. 2009, 9, 666.

16. Wu, S. W.; Myers, D. J.; Johnson, L. A. Factors affecting yield and composition of zein extracted from commercial corn gluten meal. *Cereal Chem*. 1997b, 74, 258−263.

17. Pomes, A. F. Zein. In Encyclopedia of Polymer Science and Technology: Plastics, Resins, Rubbers, Fibers; Mark, H. F.; Gaylord, N. G.; Bikales, N. M., Eds.; New York: Interscience Publishers, 1971; Vol. 15, pp 125−132.

18. Argos, P.; Pedersen, K.; Marks, M. D.; Larkins, B. A. A structural model for maize zein proteins. *J. Biol. Chem*. 1982, 257, 9984−9990.

19. Momany, F. A.; Sessa, D. J.; Lawton, J. W.; Selling, G. W.; Hamaker, S. A. H.; Willett, J. Structural Characterization of α-Zein. *J. Agric. Food Chem*. 2005, 54, 543−547.

20. Deo, N.; Jockusch, S.; Turro, N. J.; Somasundaran, P. "Surfactant Interactions with Zein Protein " *Langmuir* **2003**, *19*, 5083-5088.

21. Nakatani, N.; Hitomi, Y.; Sakaki, S. Multistate CASPT2 Study of Native Iron(III)-Dependent Catechol Dioxygenase and Its Functional Models: Electronic Structure and Ligand-to-Metal Charge-Transfer Excitation. *J. Phys. Chem. B* **2011,** *115,* 4781-4789.

22. Chowdhury, A.; Peteanu, L. A.; Holland, P. L.; Tolman, W. B. The Electronic Properties of a Model Active Site for Blue Copper Proteins As Probed by Stark Spectroscopy. *J. Phys. Chem. B* **2002,** *106,* 3007-3012.

23. Konkle, M. E.; Muellner, S. K.; Schwander, A. L.; Dicus, M. M.; Pokhrel, R.; Britt, R. D.; Taylor, A. B.; Hunsicker-Wang, L. M. Effects of PH on the Rieske Protein From Thermus Thermophilus: A Spectroscopic and Structural Analysis. *Biochemistry* **2009,** *48,* 9848-9857.

24. Khullar, P.; Singh, V.; Mahal, A.; Kaur, H.; Singh, V.; Banipal, T. S.; Kaur, G.; Bakshi, M. S. Tuning the Shape and Size of Gold Nanoparticles With Triblock Polymer Micelle Structure Transitions and Environments. *J. Phys. Chem. C* **2011,** *115,* 10442-10454.

25. Khullar, P.; Mahal, A.; Singh, V.; Banipal, T. S.; Kaur, G.; Bakshi, M. S. How PEO-PPO-PEO Triblock Polymer Micelles Control the Synthesis of Gold Nanoparticles: Temperature and Hydrophobic Effects. *Langmuir* **2010,** *26,* 11363-11371.

26. Steiner, R. F.; Kolinski, R. Phosphorescence of Oligopeptides Containing Tryptophan and Tyrosine. *Biochemistry* **1968,** *7,* 1014-1018.

27. Meyers, M. L.; Seybold, P. G. Effects of External Heavy Atoms and Other Factors on the Room-Temperature Phosphorescence and Fluorescence of Tryptophan and Tyrosine. *Anal. Chem.* **1979,** *51,* 1609-1612.

28. Timperman, A. T.; Oldenburg, K. E.; Sweedler, J. V. Native Fluorescence Detection and Spectral Differentiation of Peptides Containing Tryptophan and Tyrosine in Capillary Electrophoresis. *Anal. Chem.* **1995,** *67,* 3421-3426.

29. Huang, W.; Vernon, L. P.; Hansen, L. D.; Bell, J. D. Interactions of Thionin From Pyrularia Pubera With Dipalmitoylphosphatidylglycerol Large Unilamellar Vesicles. *Biochemistry* **1997,** *36,* 2860-2866.

30. Dasgupta, A.; Udgaonkar, J. B. Transient Non-Native Burial of a Trp Residue Occurs Initially During the Unfolding of a SH3 Domain. *Biochemistry* **2012,** *51,* 8226-8234.

31. Toca-Herrera, J. L.; Kupcu, S.; Diederichs, V.; Moncayo, G.; Pum, D.; Sleytr, U. B. Fluorescence Emission Properties of S-Layer Enhanced Green Fluorescent Fusion Protein As a Function of Temperature, PH Conditions, and Guanidine Hydrochloride Concentration. *Biomacromolecules* **2006,** *7,* 3298-3301.

32. Ragu, M.; Brnjas-Kraljevi, J. Resolved Fluorescence Emission Spectra of PRODAN in Ethanol/Buffer Solvents. *J. Chem. Inf. Model.* **2005,** *45,* 1636-1640.

33. Hou, Y.; Ye, J.; Gui, Z.; Zhang, G. Temperature-Modulated Photoluminescence of Quantum Dots. *Langmuir* **2008,** *24,* 9682-9685.

34. Singh-Rachford, T. N.; Lott, J.; Weder, C.; Castellano, F. N. Influence of Temperature on Low-Power Upconversion in Rubbery Polymer Blends. *J. Am. Chem. Soc.* **2009,** *131,* 12007-12014.

35. Zhang, D; Neumann, O.; Wang, H.; Yuwono, V. M.; Barhoumi, A.; Perham, M.; Hartgerink, J. D.; Wittung-Stafshede, P.; Halas, N. J. Gold Nanoparticles Can Induce the Formation of Protein-based Aggregates at Physiological pH, *Nano Lett*. **2009**, *9*, 666.

36. de Groot, N. S.; Ventura, S. Amyloid fibril formation by bovine cytochrome c. *Spectroscopy* **2005**, *19*, 199.

37. Pertinhez, T. A.; Bouchard, M.; Tomlinson, E. J.; Wain, R.; Ferguson, S. J.; Dobson, C. M.; Smith, L. J. Amyloid fibril formation by a helical cytochrome *FEBS Lett*. **2001**, *495*, 184.

38. Hanrahan, K. L.; Macdonald, S. M.; Roscoe, S.G. An electrochemical study of the interfacial and conformational behaviour of cytochrome *c* and other heme proteins. *Electrochim. Acta* **1996**, *41*, 2469.

39. Mueller, H.; Butt, H. J.; Bamberg, E. Adsorption of Membrane-Associated Proteins to Lipid Bilayers Studied With an Atomic Force Microscope: Myelin Basic Protein and Cytochrome c. *J. Phys. Chem. B* **2000,** *104,* 4552-4559.

40. Hinderliter, A.; Almeida, P. F. F.; Creutz, C. E.; Biltonen, R. L. Domain Formation in a Fluid Mixed Lipid Bilayer Modulated Through Binding of the C2 Protein Motif. *Biochemistry* **2001,** *40,* 4181-4191.

41. Kasbauer, M.; Bayerl, T. M. Formation of Domains of Cationic or Anionic Lipids in Binary Lipid Mixtures Increases the Electrostatic Coupling Strength of Water-Soluble Proteins to Supported Bilayers. *Biochemistry* **1999,** *38,* 15258-15263.

42. Parui, P. P.; Deshpande, M. S.; Nagao, S.; Kamikubo, H.; Komori, H.; Higuchi, Y.; Kataoka, M.; Hirota, S. Formation of Oligomeric Cytochrome c During Folding by Intermolecular Hydrophobic Interaction Between N- and C-Terminal α-Helices. *Biochemistry* **2013,** *52,* 8732-8744.

43. Joseph, D.; Geckeler, K. E. Surfactant-Directed Multiple Anisotropic Gold Nanostructures: Synthesis and Surface-Enhanced Raman Scattering. *Langmuir* **2009,** *25,* 13224-13231.

44. Tang, X. L.; Jiang, P.; Ge, G. L.; Tsuji, M.; Xie, S. S.; Guo, Y. J. Poly(N-Vinyl-2-Pyrrolidone) (PVP)-Capped Dendritic Gold Nanoparticles by a One-Step Hydrothermal Route and Their High SERS Effect. *Langmuir* **2008,** *24,* 1763-1768.

45. Dobrovolskaia, M. A.; Clogston, J. D.; Neun, B. W.; Hall, J. B.; Patri, A. K.; McNeil, S. E. " Method for Analysis of Nanoparticle Hemolytic Properties In Vitro" *Nano Lett.* **2008**, *8*, 2180-2187.

46. Zhao, Y.; Sun, X.; Zhang, G.; Trewyn, B. G.; Slowing, I. I.; Lin, V. S. Y." Interaction of mesoporous silica nanoparticles with human red blood cell membranes: size and surface effects" *ACS Nano* **2011**, *5*, 1366-1375.

47. Yu, T.; Malugin, A.; Ghandehari, H. Impact of Silica Nanoparticle Design on Cellular Toxicity and Hemolytic Activity. *ACS Nano* **2011,** *5,* 5717-5728.

48. Harbhajan Singh. *Mycoremediation: Fungal Bioremediation*. John Wiley & Sons, Nov 17, **2006**, p. 509-512.

49. Ryan K. Plague and Other Bacterial Zoonotic Diseases. In: Sherris J.C., Ryan K.J., Ray C.G. (eds) *Medical Microbiology: An Introduction to Infectious Diseases*. Fourth Edition. McGraw-Hill, USA, **2004**, 481–491

50. Mitic-Ćulafic, D.; Vukovic-Gacic, B.; Knezevic-Vukcevic, J.; Stankovic, S. Simic, Comparative study on the antibaCterial aCtivity of volatiles from sage (Salvia officinaliS l.). D. *Arch. Biol. Sci.* **2005**, *57*, 173-178.

51. Fromtling, R. A.; Galgiani, J. N.; Pfaller, M. A.; Espinel-Ingroff, A.; Bartizal, K. F.; Bartlett, M. S.; Body, B.; Frey, A. C.; Hall, G.; Roberts, G. D.; Nolte, F. B.; Odds, F. C.; Rinaldi, M. G.; Sugar, A. M.; Villareal, K. Multicenter evaluation of a broth macrodilution antifungal susceptibility test for yeasts. *Antimicrob. Agents Chemother*. **1993**, *37*, 39-45.

Figure Caption

Fig 1. (a) UV-visible scans of a reaction of aqueous zein + BSA (x_{BSA} = 0.24) with $HAuCl_4$ = 1 mM under the effect of temperature variation from 20 – 70 ^oC showing three prominent absorptions at 280 nm, 310 nm, and 540 nm. Inset represents the same reaction without $HAuCl_4$ with temperature independent effect. (b) Shows the variation in intensity of peaks 310 nm and 540 nm, along with the variation in the wavelength of 540 nm peak. (c) Steady state fluorescence of the same reaction with and without (inset) $HAuCl_4$ = 0.25 mM when excited at 280 nm with emission at 308 nm. (d) Depicts the variation in the emission intensity of proteins of different reactions of x_{BSA} = 0.24 with and without gold salt and compared with that of the reactions of pure protein components.

Fig 2. (a) Plots of nucleation temperature (N_T) and unfolding temperature (U_T) for various mole fractions of zein + BSA covering the whole mole fraction range in the presence of $HAuCl_4$. Dotted line indicates the ideal mixing. (b) UV-visible scans of a reaction of aqueous zein + BSA (x_{BSA} = 0.24) with $HAuCl_4$ = 1 mM under the effect of reaction time at constant 70 ^oC with prominent peak at 540 nm due to the formation of Au NPs. "Blank" scan indicated by the dotted line represents the absorbance of aqueous protein solution before adding gold salt. (c) Shows the variation in the intensity of 540 nm peak of Au NPs with reaction time for various zein + BSA mixtures over the entire mole fraction range. Breaks in the few plots represent the time where 540 nm peak intensity tends to constant suggesting the completion of the reaction. (d) The latter time for each mole fraction of this mixture is plotted against the mole fraction to demonstrate its dependence on their entire mixing range.

Fig 3. (a) TEM images of the purified Au NPs coated with zein prepared from aqueous zein + $HAuCl_4$ = 1 mM reaction. (b) Image of protein coated NPs prepared from aqueous zein + BSA (x_{BSA} = 0.1) with $HAuCl_4$ = 1 mM reaction. (c) and (d), TEM images of NPs prepared with mole fraction x_{BSA} = 0.24, and (e) and (f) of x_{BSA} = 0.56. Block arrows indicate thick protein coating on the NPs.

Fig 4. (a) UV-visible scans of an aqueous mixture of zein + Cyc,c ($x_{Cyc,c}$ = 0.53) without $HAuCl_4$ under the effect of temperature variation from 20 – 70 ^oC showing three prominent absorptions at 280 nm, 400 nm, and 520 nm. (b) Same reaction in the presence of $HAuCl_4$ = 1 mM with several

prominent peaks whose detail is provided in the text. (c) Depicts the variation in intensity of 310 nm, 385 nm, and 540 nm absorbances of reaction (b) with temperature. (d) Steady state fluorescence of zein + Cyc,c ($x_{Cyc,c}$ = 0.53) with $HAuCl_4$ = 0.25 mM under the effect of temperature variation from 20 – 70 ^oC when excited at 280 nm with emission at 308 nm.

Fig 5. (a) Plots of the variation in the protein emission intensity of reactions of zein + Cyc,c ($x_{Cyc,c}$ = 0.53) with $HAuCl_4$ = 0.25 mM and without $HAuCl_4$. Protein adsorption on the Au NPs in the former case depicts the non-linear variation in contrast to the latter in the absence of Au NPs. (b) Variation of the nucleation temperature (N_T) evaluated from 310 nm, 385 nm, and 540 nm absorbance peaks and unfolding temperature (U_T) from 308 nm emission peak for various mole fractions of zein + Cyc,c covering the whole mole fraction range in the presence of $HAuCl_4$.

Fig 6. (a) TEM images of Au NPs prepared from aqueous zein + Cyc,c ($x_{Cyc,c}$ = 0.16) with $HAuCl_4$ = 1 mM reaction. (b) NPs prepared with mole fraction $x_{Cyc,c}$ = 0.53. (c), (d) Images of mole fraction $x_{Cyc,c}$ = 0.72, and (e), (f) of $x_{Cyc,c}$ = 0.87. Dendritic nature of the NPs increases with the increase in the amount of Cyc,c in the zein + Cyc,c mixtures due to the poor shape control effects.

Fig 7. Schematic representation of possible complex formation in zein + BSA (a) and zein + Cyc,c (b) mixtures based on Fig 2 and 5, respectively, due to electrostatic interactions between the hydrophilic domains of respective components. (c) The complex formation in zein + BSA driven by the hydrophobic interactions operating between the hydrophobic domains. (d) Depicts the self – aggregation in Cyc,c.

Fig 8. (a) Absorbance profiles of hemolysis exhibited by different doses of Au NPs prepared with a reaction of mole fraction $x_{Cyc,c}$ = 0.53. Photos show the extent of hemolysis for these samples with +ive and -ive controls. (b) Variation in the percentage hemolysis by Au NPs with different doses prepared over the entire mole fraction of zein + BSA (empty symbols) and zein + Cyc,c (filled symbols) mixtures. (c) Schematic depiction of the effect of shape, size, and protein coating on the hemolysis. Roughly spherical small NPs coated with protein cannot induce hemolysis in comparison to large dendritic NPs without protein coating. See text for details.

Fig 9. Plots of minimum inhibitory concentration (MIC) of protein coated Au NPs of zein + BSA (a) and zein + Cyc,c (b) mixtures over the whole mole fraction range for Asperagillus niger (B), Candidum geotrichum (C), Candida albicans (D) and Candida tropicalis (E). Dotted lines in both figures represent the MIC for antifungal drug “Fluconazole” as control.

Fig 1

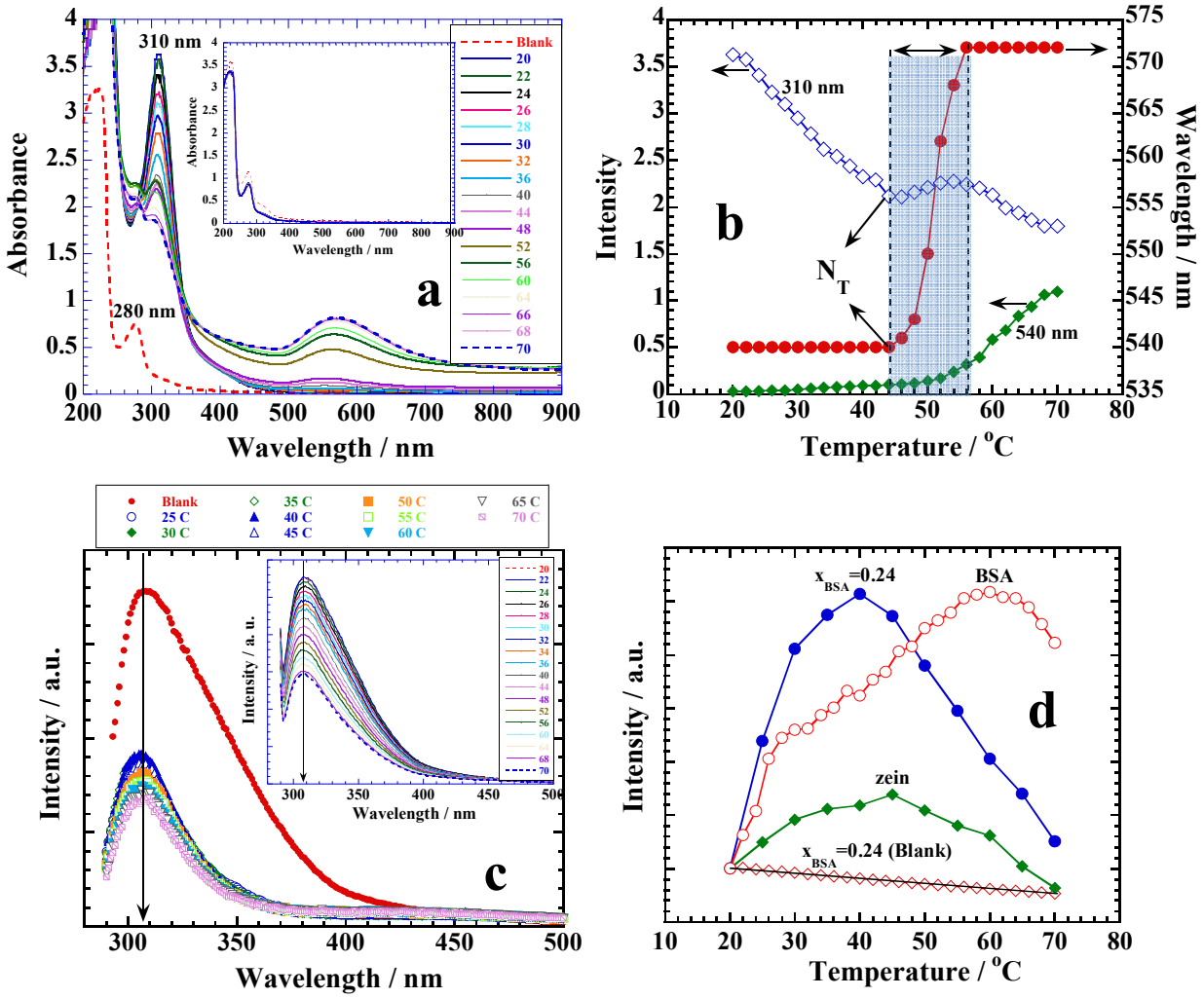
a
Absorbance
Wavelength / nm
310 nm
280 nm
Blank
20
22
24
26
28
30
32
36
40
44
48
52
56
60
64
66
68
70
b
Intensity
Wavelength / nm
Temperature / °C
310 nm
540 nm
N T
c
Intensity / a.u.
Wavelength / nm
Blank
25 C
30 C
35 C
40 C
45 C
50 C
55 C
60 C
65 C
70 C
d
Intensity / a.u.
Temperature / °C
x BSA =0.24
BSA
zein
x BSA =0.24 (Blank)

Fig 2

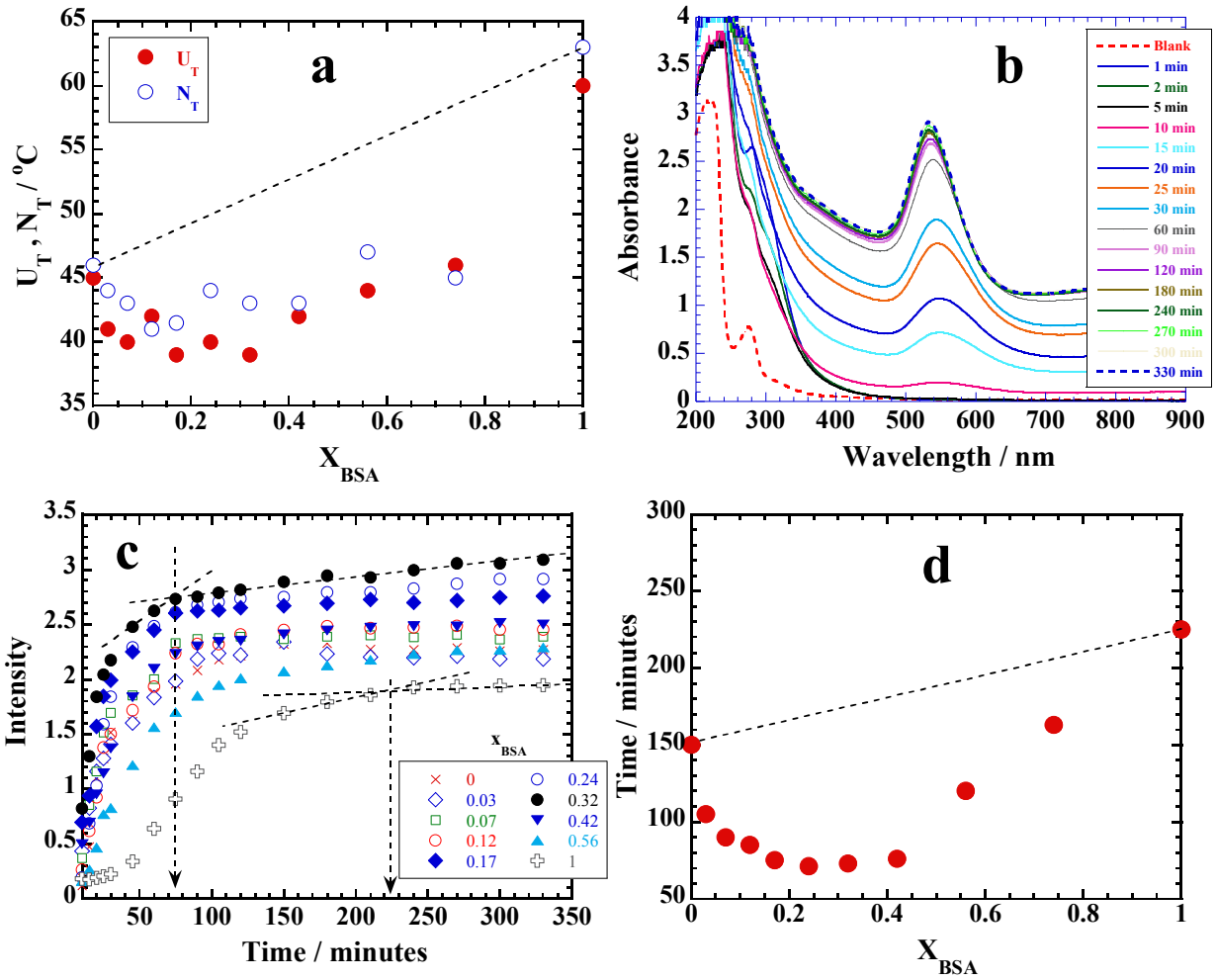
a
U_T
N_T
U_T, N_T / °C
X_{BSA}
b
Absorbance
Wavelength / nm
Blank
1 min
2 min
5 min
10 min
15 min
20 min
25 min
30 min
60 min
90 min
120 min
180 min
240 min
270 min
300 min
330 min
c
Intensity
Time / minutes
X_{BSA}
0
0.03
0.07
0.12
0.17
0.24
0.32
0.42
0.56
1
d
Time / minutes
X_{BSA}

Fig 3

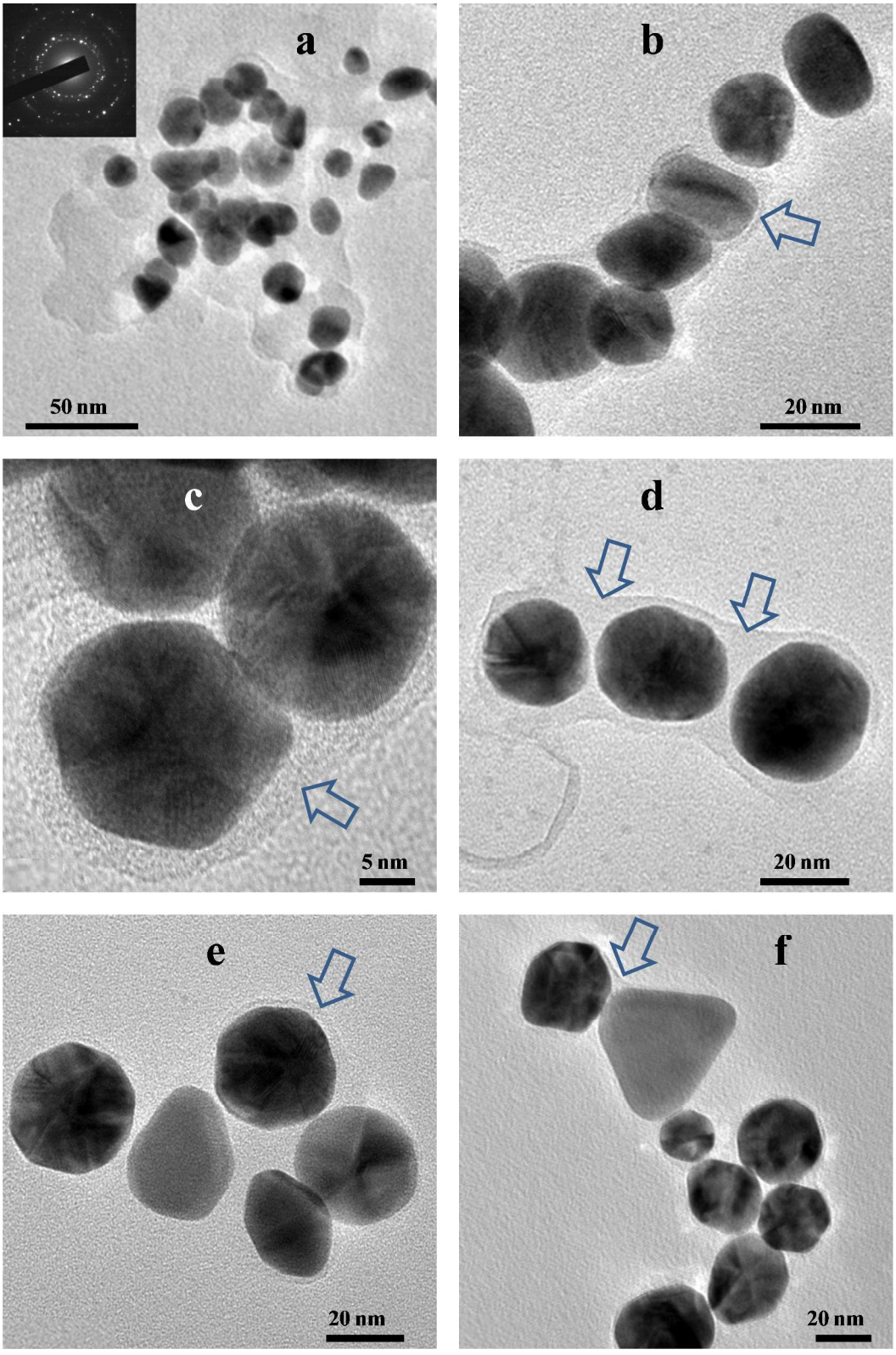

Fig 4

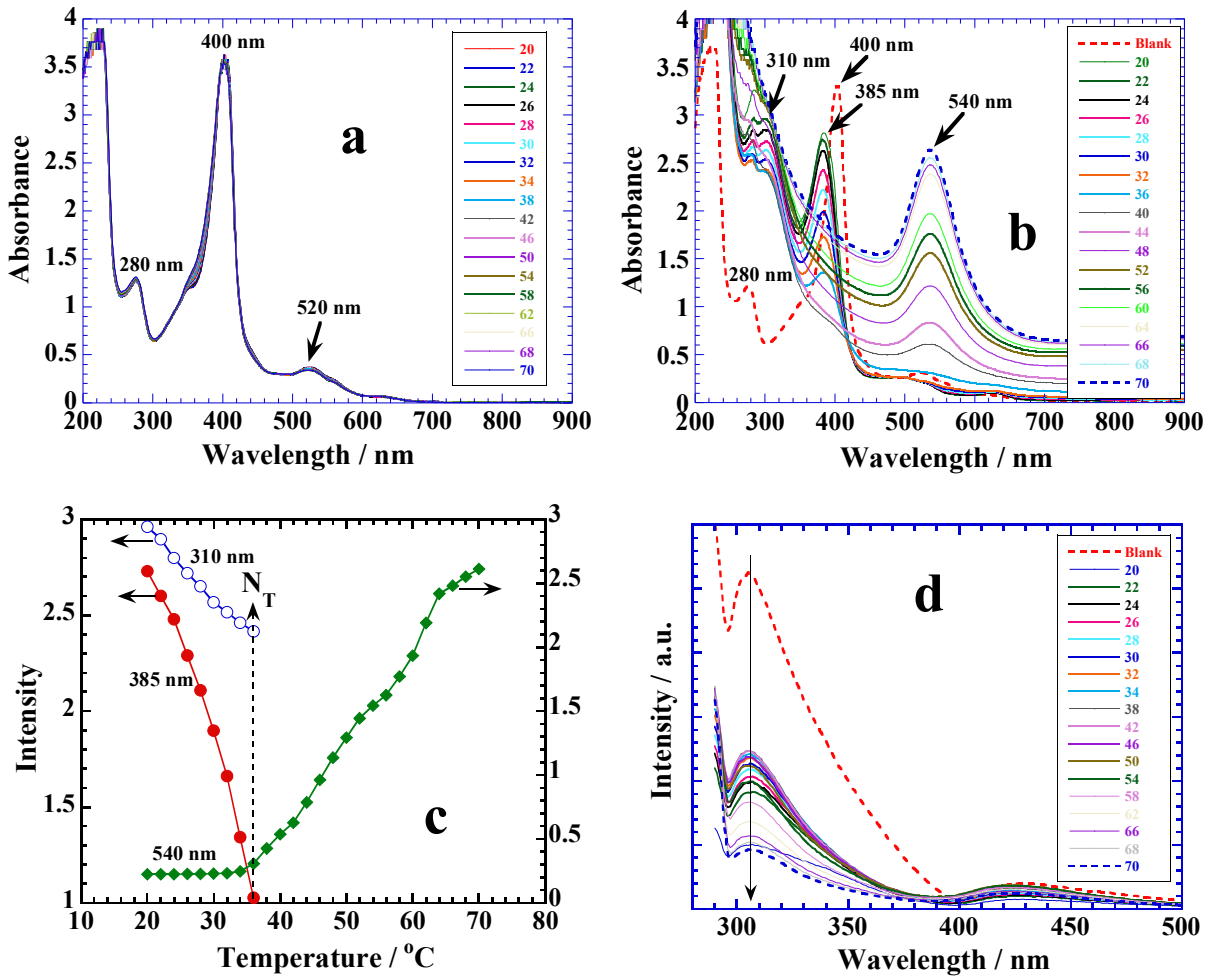
a
Absorbance
Wavelength / nm
400 nm
280 nm
520 nm
b
310 nm
385 nm
540 nm
Blank
c
Intensity
Temperature / °C
N_T
d
Intensity / a.u.

Fig 5

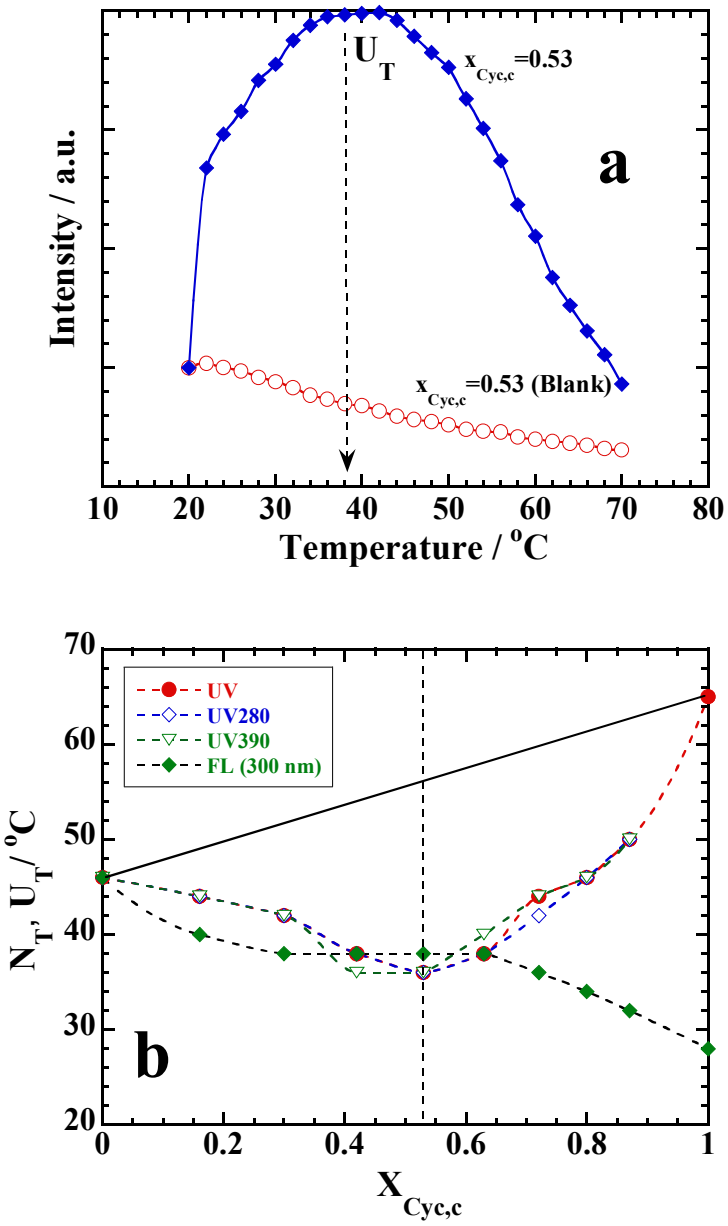
Intensity / a.u.
Temperature / °C
U_T
x_Cyc,c=0.53
x_Cyc,c=0.53 (Blank)
a
b
UV
UV280
UV390
FL (300 nm)
N_T, U_T / °C
X_Cyc,c

Fig 6

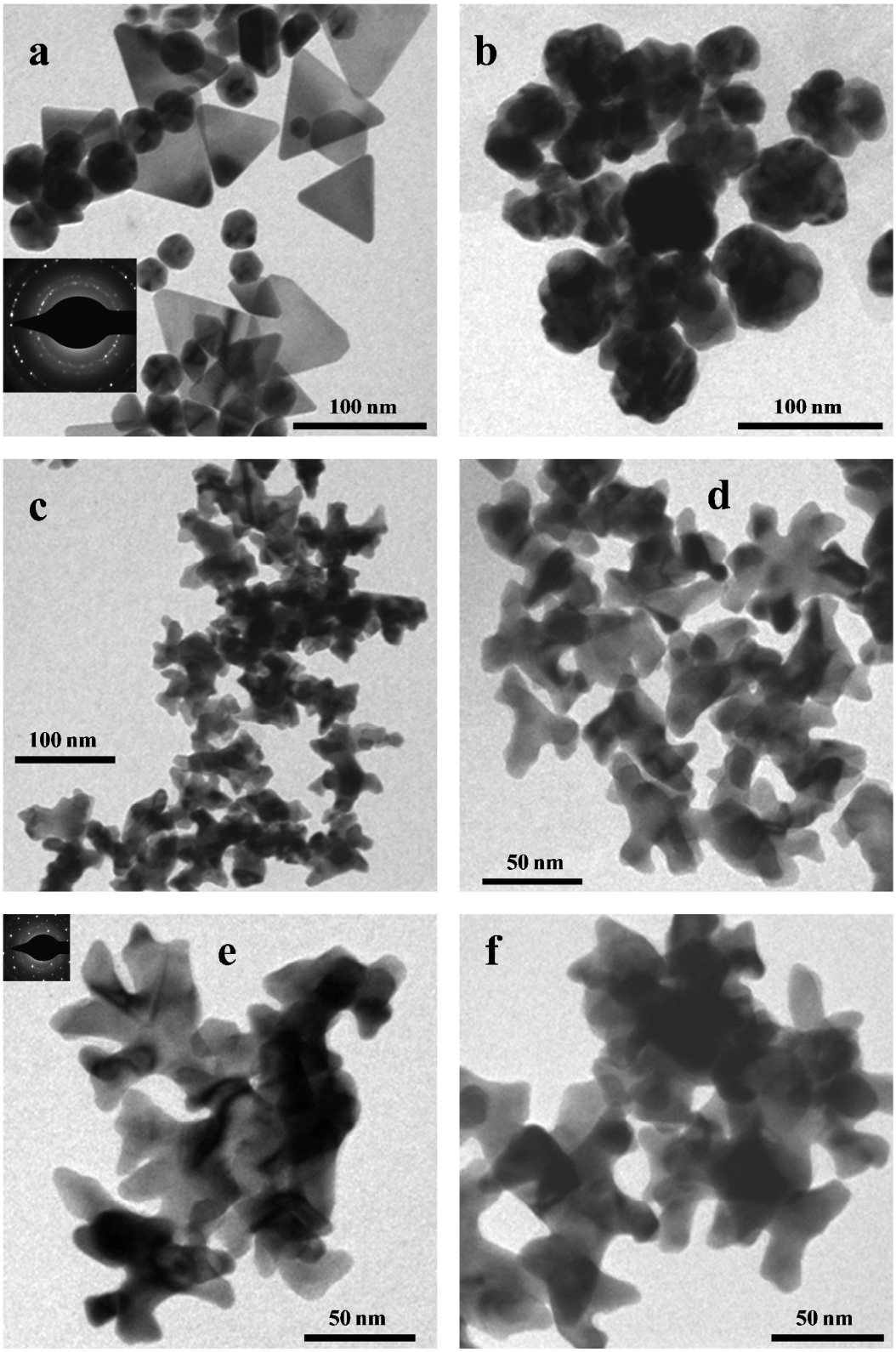

Fig 7

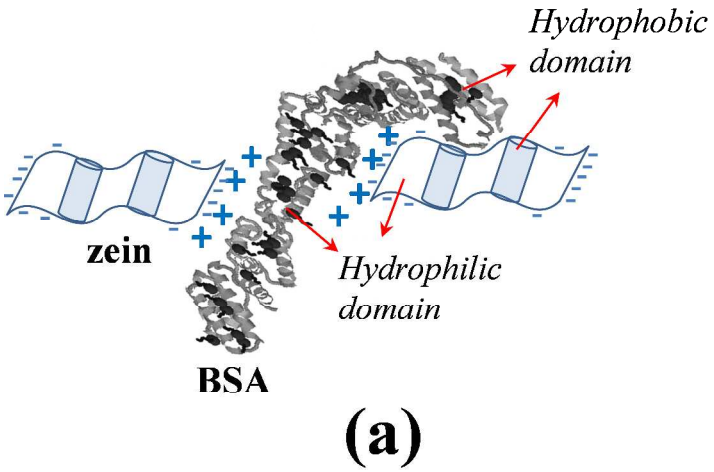

(a)

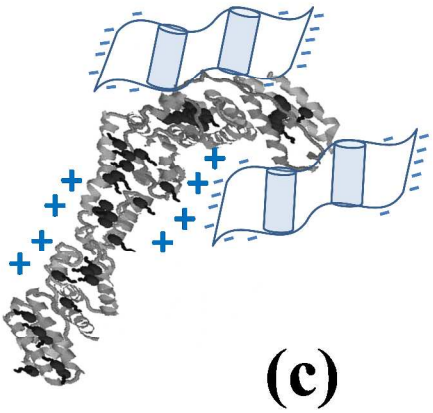

(c)

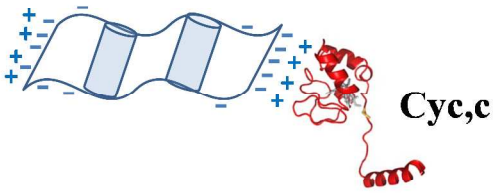

(b)

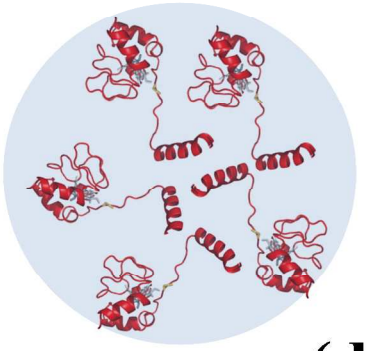

Self - aggregation **(d)**

Fig 8

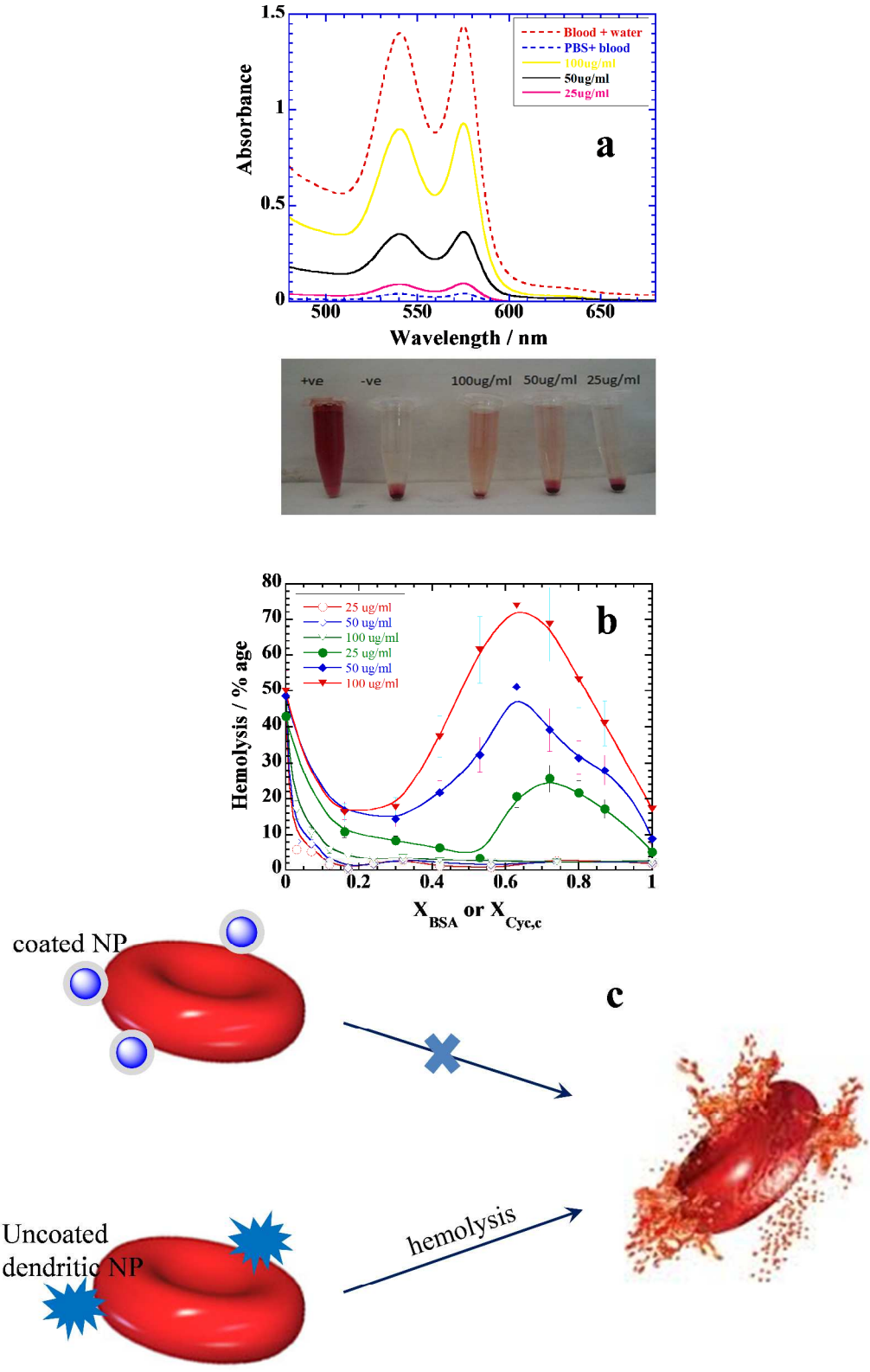
Absorbance
Wavelength / nm
Blood + water
PBS+ blood
100ug/ml
50ug/ml
25ug/ml
a
+ve
-ve
100ug/ml
50ug/ml
25ug/ml
Hemolysis / % age
25 ug/ml
50 ug/ml
100 ug/ml
25 ug/ml
50 ug/ml
100 ug/ml
b
X BSA or X Cyc,c
coated NP
c
Uncoated
dendritic NP
hemolysis

Fig 9

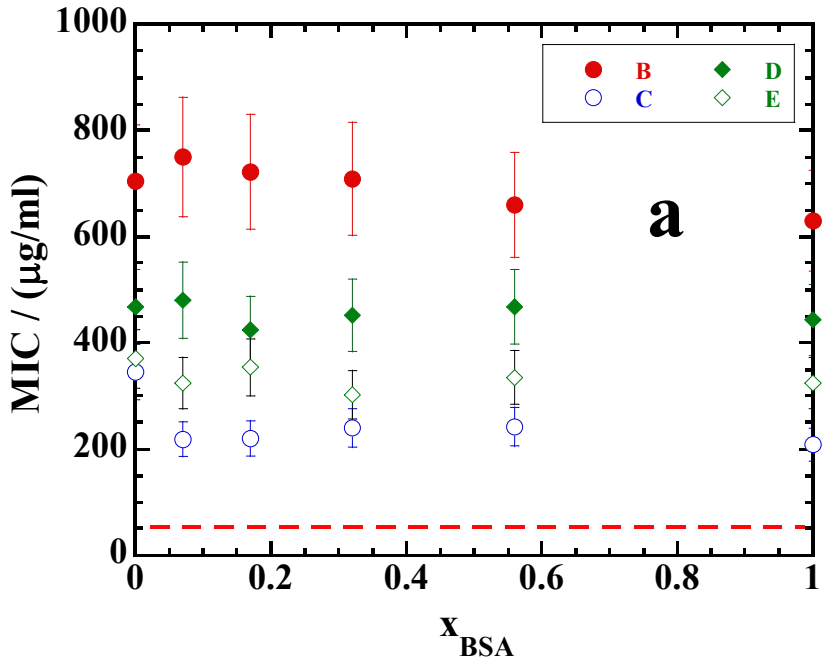
1000
800
600
400
200
0
MIC / (μg/ml)
0
0.2
0.4
0.6
0.8
1
x BSA
B
C
D
E
a

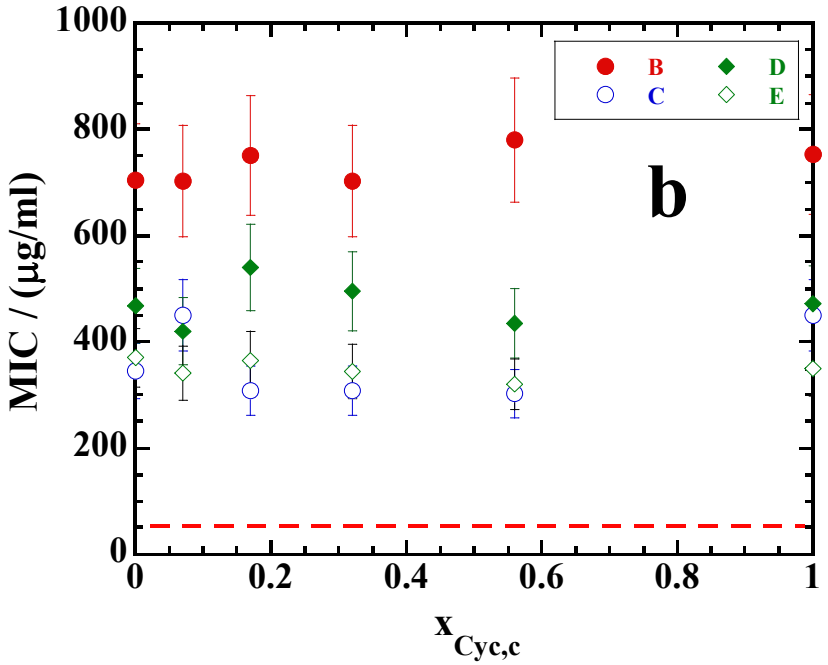
1000
800
600
400
200
0
MIC / (μg/ml)
0
0.2
0.4
0.6
0.8
1
x Cyc,c
B
C
D
E
b

Protein Mixtures of Environmental Friendly Zein to understand Protein – Protein Interactions through Biomaterials Synthesis, Hemolysis, and their Antimicrobial Activities

Aabroo Mahal, Manoj Kumar, Poonam Khullar, Harsh Kumar, Narinder Singh, Gurinder Kaur, Mandeep Singh Bakshi

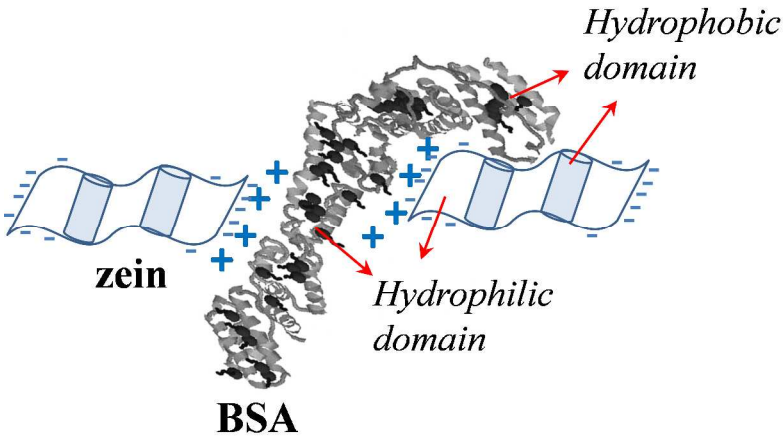

Protein – protein interactions through biomaterials synthesis for biological applications.